Chapter 9

Shale Gas in Poland

Jadwiga A. Jarzyna, Maria Bała,
Paulina I. Krakowska, Edyta Puskarczyk,
Anna Strzępowicz, Kamila Wawrzyniak-Guz,
Dariusz Więcław and Jerzy Ziętek

Additional information is available at the end of the chapter

http://dx.doi.org/10.5772/67301

Abstract

An example of interpretation of the Silurian and Ordovician shale formations in the Baltic Basin in Poland regarding determination of potential sweet spots is presented. Short geological information shows the position of shale gas play. Description of the data—laboratory measurement outcomes (petrophysical and geochemical) and well logging—presents results available for analyses. Detailed elemental analyses and various statistical classifications show the differentiation between sweet spots and adjacent formations. Elastic property modelling based on the known theoretical models and results of comprehensive interpretation of well logs is a good tool to complete information, especially in old wells. Acoustic emission investigations show additional characteristic features of shale gas rock and reveal that acoustic emission and volumetric strain of a shale sample induced by the sorption processes are lower for shale than for coals.

Keywords: shale gas, petrophysics and well logging, statistical analyses, acoustic emission, Baltic Basin

1. Introduction

Shale gas deposits belong to unconventional hydrocarbon resources. Nowadays, unconventional resources (tight gas, shale gas) are under careful and detailed consideration regarding cognitive works. The world is interested in prospection of unconventional deposits because of the necessity to increase energy resource production and geological limitations regarding conventional deposits. Also, economical aspects are important. Interest in shale gas arises when prices of hydrocarbons are high. In conventional oil and gas deposits, mature rock,

reservoir and sealing rock are crucial. Also, geological traps enabling accumulation of hydrocarbons are important. Traditional prospecting by seismic methods and well logging is oriented to find traps and good reservoirs—high porosity and high permeability rocks enabling fluid flow. In shale gas, prospection source and reservoir rock are the same formation. Finding of shale formations is easier than conventional traps, but exploitation of hydrocarbons due to low porosity and very low permeability is more difficult. In shale gas, plays information on rock elastic properties is a crucial issue. An additional element complicating the unconventional shale gas reservoir model is dispersed organic matter (kerogen). New technologies are elaborated to make prospection of shale gas deposit more efficient.

In the paper, there are presented results of laboratory measurements and well logging obtained using conventional (i.e. resistivity and density and acoustic gamma ray logs) and selected modern methods (i.e. geochemical and NMR logs). The goal of the paper is presentation of available method application on contouring and characterization of sweet spots (differentiation between parts of the formation rich in hydrocarbons and surrounding rocks). An example of data interpretation of the Silurian- and Ordovician-age shale formations in the Baltic Basin in Poland is presented.

2. Selected geological information about Polish shale gas formations

In the Polish sedimentary basins beginning with the Baltic Basin in the north (**Figure 1**) to the Lublin Basin in the southeast part of Poland, there are numerous siltstone and mudstone deposits, rich in oil-prone organic matter (Type II kerogen).

Shale rocks, rich in organic matter, may be the exploration targets in terms of unconventional hydrocarbon (oil and gas) reservoirs [3–5]. Silurian and Ordovician shales in Poland spread along the western margin of the East European Platform in Lublin, Podlasie and Baltic basins, reaching about 700 km in length [6]. On Łeba elevation where the exemplary boreholes (L-1, K-1, O-2, B-1 and W-1) are located, the sedimentation, organic-rich black shales where the graptolites are the main fossil, started in the Late Llanwirnian reaching Wenlock [7].

The object of the analysis covers two formations, being potentially resources of unconventional hydrocarbons: Ja Member of the Silurian Pa formation and Ordovician Sa formation. Silurian Pa Fm was firstly described by Tomczyk [8]. The formation lithostratotype is the part of the Ko IG-1 well profile. In analyzed wells, the Pa formation is placed between Pr Fm (lower boundary) and Pe Fm (upper boundary). The lower boundary is marked at the point of clear lithological changes involving the replacement of limestone or marl deposits of Ordovician series into clay sediments of the Pa formation. It is clearly visible on the well logs. The lower part of the formation is built by black, bituminous claystones passing to the top into dark grey claystones, laminated by greenish, grey-greenish and black claystones or brown calcareous claystones and bentonite laminas. These sediments contain very large and diverse taxonomic graptolite groups [7, 9]. Sedimentation environment of these strata may be compared with clays/marls formed in the central part of the open or periodically isolated epicontinental shelf with the dominance of environment where coarse-grained material was rarely delivered. An average thickness of the

http://dx.doi.org/10.5772/67301

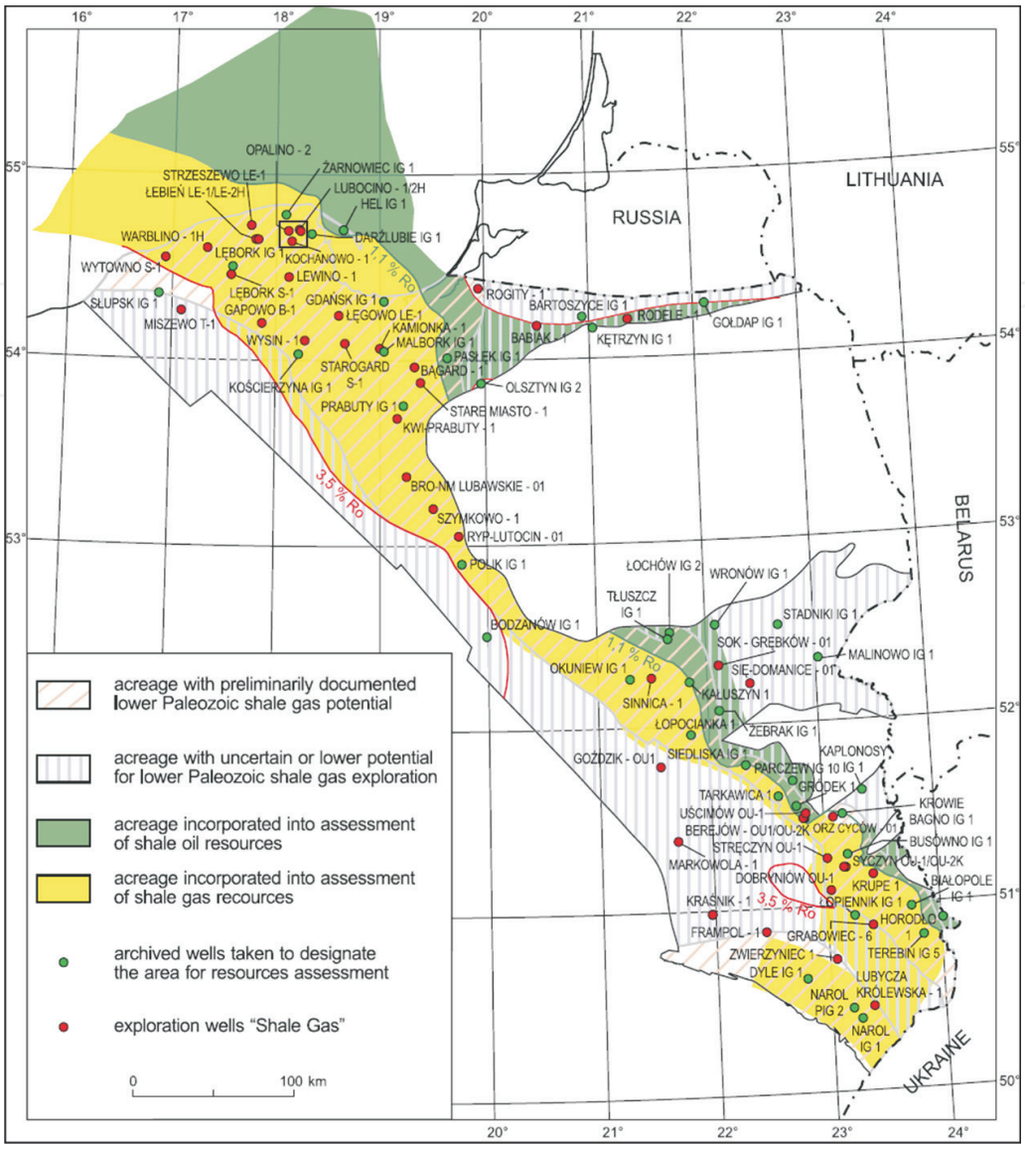

Figure 1. Occurrence of the lower palaeozoic fine-grained rocks potentially accumulating shale gas. Small rectangle—study area ([1] modified, [2]).

Pa Fm is 20–40 m increasing from east to west and not exceeding 70 m [10]. Ja Mb belongs to the lower part of the Pa Fm and is built of black bituminous claystones. It is characterized by high organic matter content; however, it may not ensure large gas reserves since the thickness of this bed does not exceed 12 m [10]. Geological profile of Gd IG-1 well is proposed as the member of lithostratotype. The lower boundary of the member is also the lower boundary of the Pa formation, while the upper boundary is marked on the profile in the place where grey and dark-grey claystones, laminated with grey-greenish and black claystones, occur. The discussed boundaries are clearly visible on the logs because of the sharp increase of natural radioactivity within the rocks. Ja Member is composed of black claystones containing commonly pyrite and high content of the oil-prone organic matter (total organic carbon (TOC) content up to 7.6 wt.% in O-2 well profile), with dark-grey calcareous laminas and few intercalations of dark-grey marly limestones.

The second object of the interest is the Sa formation, which was fully described by Modliński and Szymański [11, 12]. The formation lithostratotype is proposed as the part of the Za IG-1 well profile. The lower boundary runs on the Ko limestone formation within Llanwirnian and Llandeilian series, while the upper boundary is set by the Pr marl and shale formation within Ashgillian series. Lithology is mainly composed of black, dark grey and grey-greenish bituminous shales (TOC up to 7.2 wt.% in B-1 well profile). In some parts of the formation, bentonite intercalations are present. Moreover, dark grey, grey and grey-greenish marly limestone and marl intercalations are visible. Organic remains, in form of graptolites, are common in this formation [7]. The thickness of the Sa formation increases from the east to west and northwest, from 3.5 to 37 m in land part of the Baltic Basin and from 26.5 to 70 m on the Baltic Sea shelf.

The differences of mineral composition between shale rocks frequently presented in the literature [13] and shale rocks in the study area are shown in **Figure 2**. In L-1 borehole, there is presented division of the Silurian and Ordovician shales into selected formations. Distinctly visible differences are the reason of slightly different approaches applied to interpretation of the Polish shale gas formations in comparison to other shale plays in the world.

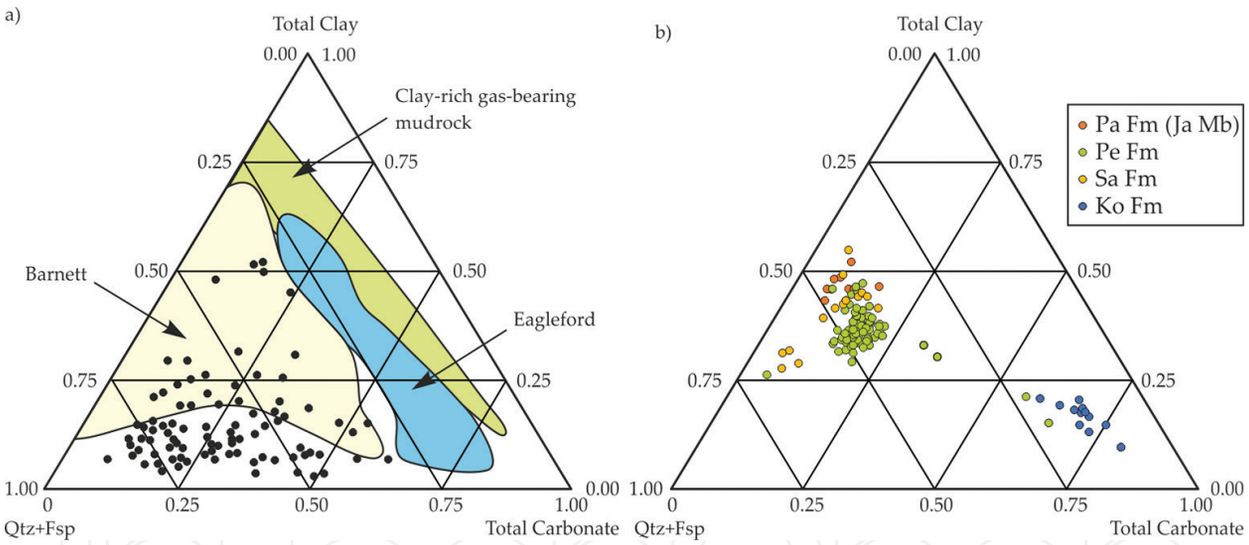

Figure 2. Mineral composition of shale gas formations: (a) well known from the literature (after Ref. [13]), black points—Thistleton reservoir; (b) Polish shales in L-1 well.

3. Petrophysical and geochemical laboratory and well-logging data to characterize shale gas formation

The research material consists of the results of petrophysical and geochemical laboratory measurements on core samples and well-logging data [14]. Data were selected as the most representative for the Silurian and Ordovician shale formations in the Baltic Basin. Three of the wells (L-1, K-1 and O-2) are located in the north part of the study area (**Figure 1**), whereas B-1 and W-1 wells are located more to the south.

http://dx.doi.org/10.5772/67301

The results of petrophysical laboratory measurements composed the dataset of density, bulk density and total porosity from helium pycnometer. Additionally, effective porosity derived from the mercury or helium porosimetry was included. Nuclear magnetic resonance spectroscopy provided information about clay-bound water, capillary-bound water, free water and also total, effective porosity and irreducible water saturation. Absolute permeability was obtained using nitrogen permeameter [14]. Presented laboratory data set is typical for both conventional and unconventional hydrocarbon reservoir investigations.

The organic geochemical analyses oriented to unconventional hydrocarbon deposits study are the same as for characterization of source rocks of conventional oil and gas accumulations. The most useful is Rock-Eval pyrolysis allowing determination inter alia contents of pyrolyzable (PC) and total organic carbon (TOC), free hydrocarbons (S1) and hydrocarbons generated through thermal cracking of non-volatile organic matter (residual hydrocarbons, S2). The temperature of hydrocarbon maximum release during kerogen cracking (Tmax) allows estimation of the thermal maturity and also calculated hydrogen (HI) and production (PI) indices may help in determination of kerogen genetic type and zones of epigenetic hydrocarbons saturation, respectively.

Shales of Sa Fm and Ja Mb are rich in organic matter with the median values of TOC amounting 3.1 and 3.0 wt.%, respectively. The highest TOC contents, 7.2 wt.% in Sa Fm and 7.6 wt.% in Ja Mb, were recorded in B-1 and O-2 well profiles, respectively. The highest TOC medians were recorded in wells located in the north-eastern part of the study area. In these profiles, hydrocarbon potential of analyzed rocks described by HI values was not high and mostly varied from 100 to 200 mg HC/g TOC for both formations. Hydrocarbon potential of Sa Fm and Ja Mb in profiles located south and west (in deeply buried parts of basin) was even lower—HI values usually did not exceed 100 mg HC/g TOC. Observed variability of Rock-Eval parameters and indices between individual profiles for both formations are result of thermal maturity changes: from middle in north-eastern to final stage of oil window in south-western part of the study area.

In the investigated wells, a set of standard logging curves along with more advanced measurements were available (i.e. cross dipole sonic and geochemical logs). Results of the comprehensive interpretation of logs were also included in the analyses [14]. Among all well-logging data, there were selected several that represented the most important properties in petrophysical description of shale formation. They were as follows: natural radioactivity represented by total (GR); spectral gamma ray logs (GRKT) (calibrated sum of the potassium and thorium energy windows); concentration of naturally occurring elemental sources (POTA, THOR, URAN); resistivity of invaded and uninvaded zones measured by shallow and deep laterologs (LLS, LLD); neutron porosity hydrogen index (NPHI); bulk density (RHOB); photoelectric absorption index (PEF) and velocity of compressional and shear waves in the formation expressed by slowness of P and S waves (DTP, DTS). Special meaning had information from geochemical logging: elemental weight fractions (Si, Ca, K, Mg, Al, Ti, Fe, Gd, S, Mn); mineral volume fraction (quartz (QRTZ), calcite (CALC), dolomite (DOLM), pyrite (PYRT), clay minerals (VCL) apart from illite (ILLI) and chlorite (MGCL) and kerogen (KERO)); volume of clay-bound water, gas and free water (CBW, VWF, VGAS); as well as total and effective porosity (PHIT, PHIE) and water saturation (SW). Described data set was not available in all wells; nevertheless, the detailed petrophysical and geochemical analyses of laboratory and well-logging data were carried out on shale gas formations.

Characteristics of the uranium content from spectral gamma ray log and TOC wt.% from laboratory measurements vs. depth in L-1 well are presented in **Figure 3a** including stratigraphy. It is distinctly visible that Ja Mb of Pa Fm and Sa Fm is different from the adjacent formations.

Transit interval time of P wave, DTP, vs. resistivity, LLDC, and bulk density, RHOB, plots confirmed different features of aforementioned beds (**Figure 3b, c**). Points from the adjacent formations (Pe Fm, Pa Fm and Pr Fm) and potential sweet spots (Ja Mb and Sa Fm) are composed of separate data sets. Resistivity and bulk density covered the bigger range in sweet spots in comparison to the surrounding formations. DTP decreased with the increase of resistivity in shale formations with limited content of organic matter. Data representing rock material of high volume of organic matter had similar and high DTP values and high resistivity (**Figure 3b**). In the same rocks, bulk density decreased due to lower density of kerogen (**Figure 3c**). Discussed formations rich in organic matter, i.e. Ja Mb of Pa Fm and Sa Fm, revealed also differences between each other.

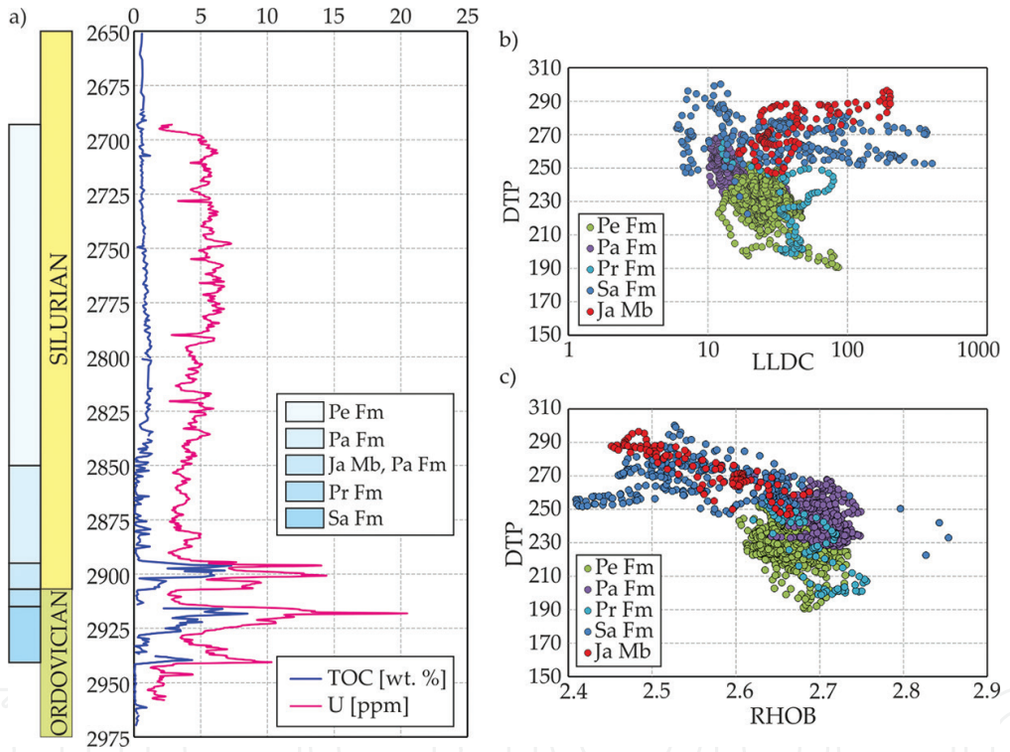

Figure 3. Distinct well log anomalies in L-1 well: (a) very dense-point laboratory TOC results and U curve from the spectral gamma log; (b) transit interval time, DTP, vs. borehole-corrected resistivity, LLDC; and (c) transit interval time, DTP, vs. bulk density, RHOB.

4. Classification of shale gas formations by statistical methods on the basis of laboratory and well-logging data

4.1. Basic statistics of laboratory data

Petrophysical and geochemical parameters from laboratory measurements were the object of analysis in order to create the model of shale gas formations in Poland. Statistical approach allowed to identify the regularities between the parameters in data set.

http://dx.doi.org/10.5772/67301

The average bulk density in L-1 well varied from 2.54 g/cm^3 in Ja Mb to about 2.67 g/cm^3 in Pr Fm. Distribution of bulk density in Pe Fm from B-1 well is presented in **Figure 4a**. In this case, bulk density concentrated in the range of 2.6–2.65 g/cm^3 in 45% of the samples. Average total porosity from pycnometer in L-1 well was equal to about 3.2% in Ko Fm to about 6.45% in Pa Fm, whereas from NMR spectroscopy from 3.28% in Ko Fm to about 8.62% in Sl Fm. Taking into consideration absolute permeability from permeameter in L-1 well in Pa Formation 75% of values was lower than 0.001 mD. In Pe Fm, the same percentage (75%) comprised plugs with permeability lower than 3.48 mD. Irreducible water saturation from NMR indicated lower values in B-1 well in comparison to L-1 well, where most of the samples were characterized with values above 85%. Average total organic carbon ranged from about 0.07 wt.% in Ko Fm to about 3.8 wt.% in Ja Mb in L-1 well (**Figure 4b**), while in B-1 well from about 0.20 wt.% in Pr Fm to about 3.37 wt.% in Ja Mb. The amount of free hydrocarbons in both wells was high in Ja Mb of Pa Fm and in Sa Fm (**Figure 4b**). Regarding mineral content in shale gas formations, Pe Formation was characterized by lower content of clay minerals and higher of quartz, calcite and dolomite than Ja Mb and Sa Fm in L-1 well. The higher amount of pyrite was observed in Pa formation, especially in Ja Mb. The presence of pyrite had a negative influence on measured parameters because it decreased the resistivity and increased density readings. Also, volume of pyrite influenced elastic properties of the rocks. The best deposit parameters (e.g. high porosity and total organic carbon) in all wells were observed in Sa Fm and Pa Fm within shale gas plays.

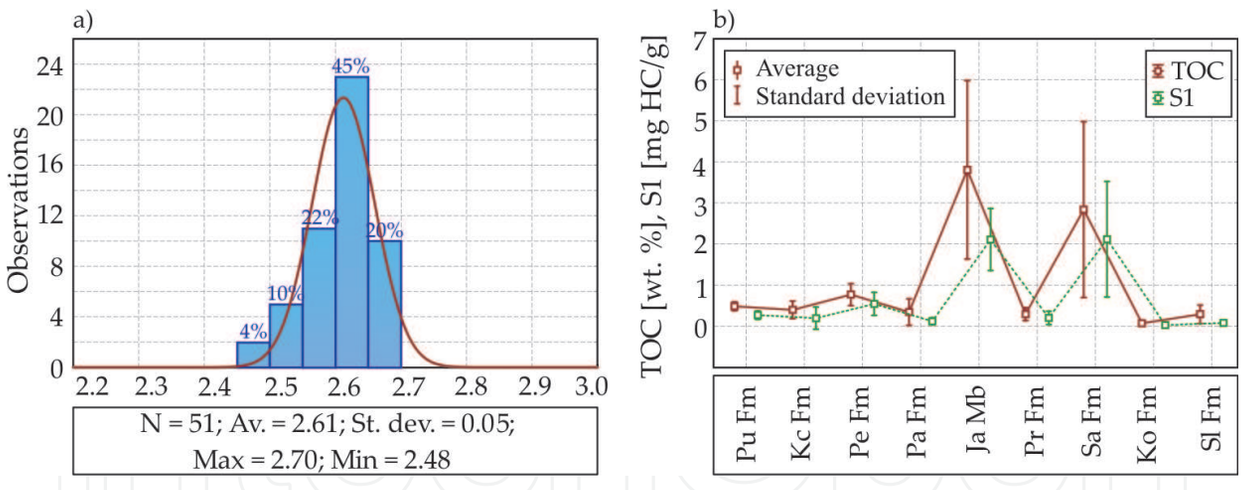

Figure 4. (a) Histogram of bulk density in Pe Formation, B-1 well. Symbols: N, number of samples; Av., average value' St. dev., standard deviation; Max, maximum value; Min, minimum value. (b) Total organic carbon (TOC) in wt.% and the amount of free hydrocarbons (S1) in % from Rock-Eval pyrolysis in various lithostratigraphic units, L-1 well.

4.2. Elemental weight percent from geochemical logging in shale classification

Geochemical logging was run over the Silurian and Ordovician intervals where geologists determined several shale formations. As a result, concentrations of 10 elements, Si, Ca, K, Mg, Al, Ti, Fe, Gd, S and Mn, were determined and utilized to characterize each formation. Statistical box plots clearly showed that the investigated shales could be grouped into three types of formation regarding distribution of the elements. The first group was composed of clayey sediments of Pu Fm and Pa Fm including Ja Mb and Sa Fm. Characteristic features of

these shale formations were very high concentration of aluminium, reduced amount of calcium and slightly increased amount of iron (**Figure 5a**). Kc Fm, Pe Fm and Pr Fm formed the second group, where mudstones were present together with claystones. A bit higher content of calcium than in the first group was observed (**Figure 5b**). Both groups had a significant amount of silicon. The third group was represented only by calcareous mudstones of Re Mb of Kc Fm. It showed the highest concentration of calcium and magnesium with the lowest amount of aluminium and decreased amount of potassium and iron when comparing to the other fine-grained sediments (**Figure 5c**). It should be pointed that the distribution of elements was very similar to elemental distribution obtained for limestones of Ko Fm. Presented box plots excluded gadolinium content due to other orders of magnitude (ppm vs. percent). The separate box plot for this element (**Figure 5d**) revealed that two formations considered as sweet spots (Ja Mb and Sa Fm) were characterized by much higher amount of Gd.

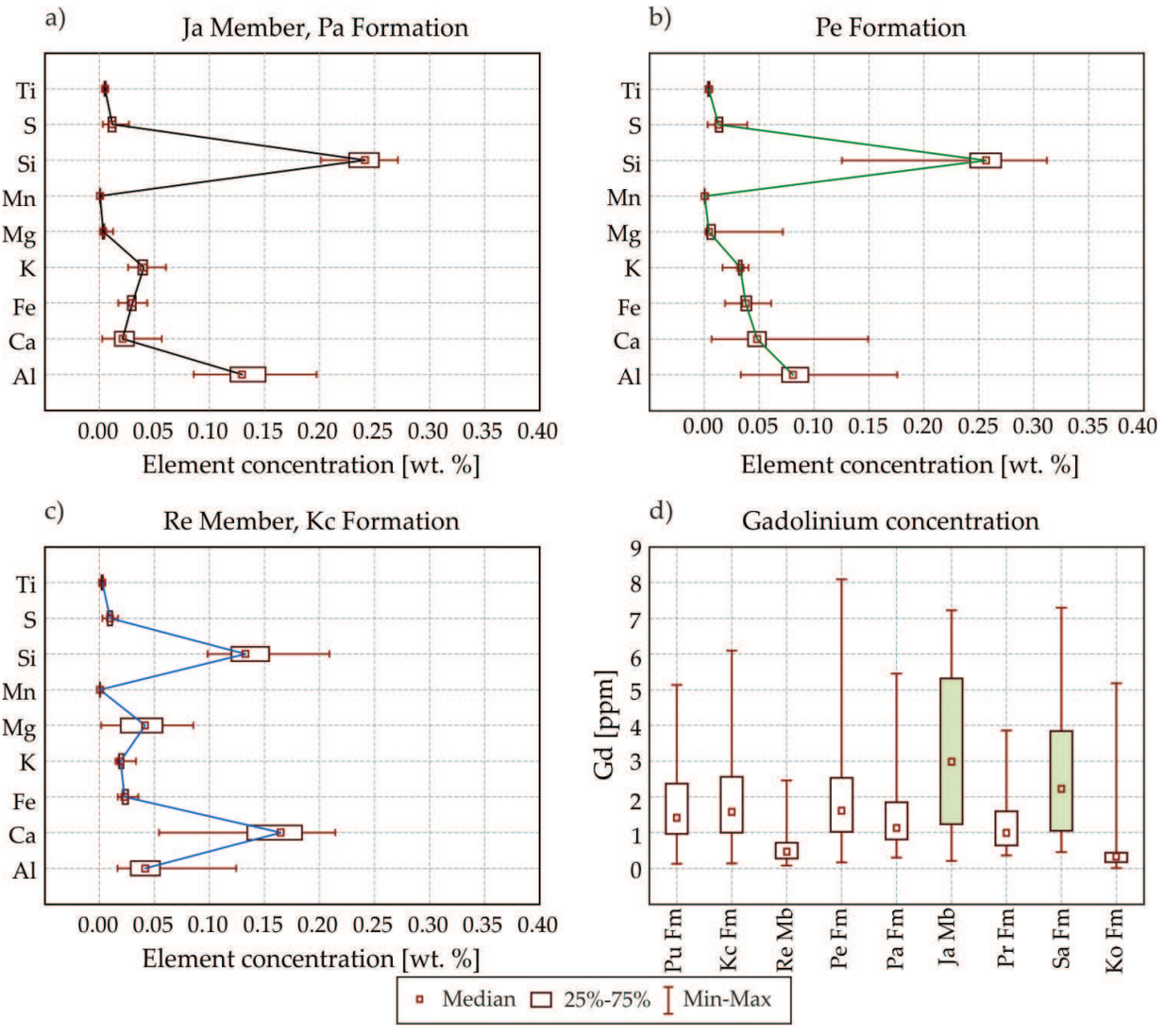

Figure 5. Box plots of elements distribution in shale formations from Baltic Basin in Poland: (a) Ja Mb and Pa Fm, (b) Pe Fm, (c) Re Mb and Kc Fm and (d) gadolinium content.

http://dx.doi.org/10.5772/67301

4.3. Heterogeneity of shale formations confirmed by factor analysis

Factor analysis (FA) was applied to logging data from three closely located wells in the Baltic Basin: L-1, O-2 and K-1. FA described a collection of observed variables (i.e. logs) in terms of a smaller collection of (unobservable) latent variables or factors. Achieving meaningful petrophysical interpretation of the logs through the factors helped to understand the complex geophysical responses of organic-rich Polish shales. The input data included parameters measured in wells, results of the comprehensive interpretation of well logs and results of elastic wave velocity and density estimations from Biot-Gassmann model [15]. FA was applied to data from each formation from each well independently and from all wells together. Results revealed very complicated nature of investigated sediments; however, some similarities were observed. For example, in Sa Fm, petrophysical properties represented by the factors were similar in each well, though a slightly different set of logs loaded the factors.

The first factor was always controlled mainly by clay and shale content, the second factor was expressed either by specific minerals (e.g. calcite or pyrite) or by elastic wave velocities and the third factor was represented by organic matter. When this formation was jointly analyzed in all the wells, results confirmed analyses done for the separate wells (**Figure 6**). However, more often diversity than similarity was observed within one formation between the wells. **Figure 7** shows results for Pa Fm from two wells. It can be seen that the appropriate factors were loaded by different logs and were represented by significantly different petrophysical parameters. The case of K-1 well showed that the most important parameters were clay content (first factor), properties of pore space, i.e. porosity and fluids volume (second factor), and organic matter (third factor). In L-1 well, petrophysical interpretation of the first factor was rather unclear, the second factor could be linked to sonic velocity controlled by shale and quartz volumes and the third factor was related to organic matter.

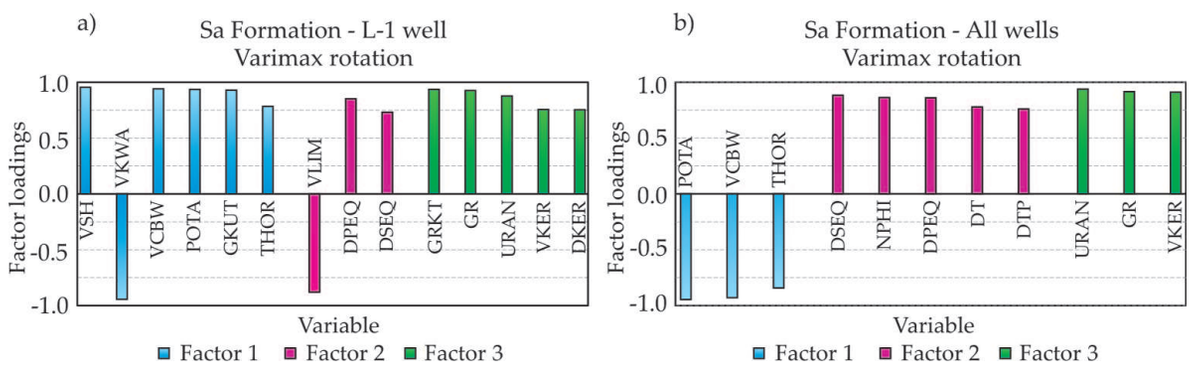

Figure 6. Factor analysis results for (a) Sa Fm in L-1 well and (b) all wells.

These examples showed that FA was useful in determination of similarities and differences of shales. Investigated formations displayed significant heterogeneity between each other, between adjacent sediments and from one well to another, but some characteristic features were also observed. FA revealed that the most significant properties in characterization of Polish shales were mineral composition, porosity and fluid volume, mechanical properties and content of organic matter.

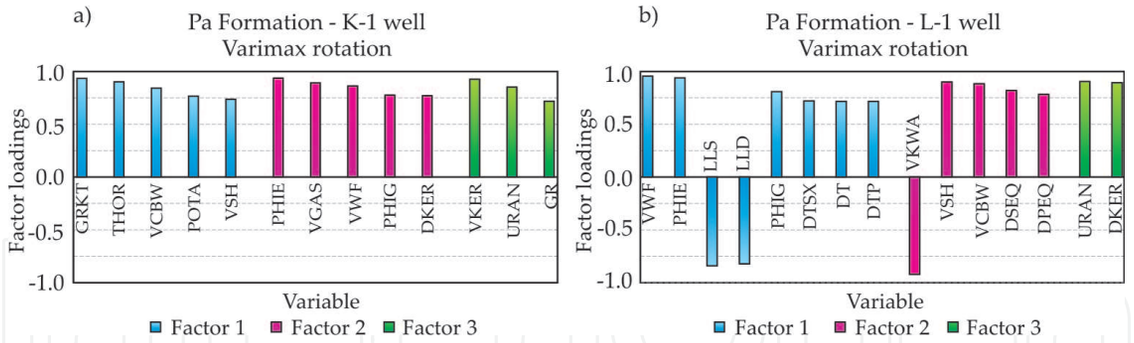

Figure 7. Factor analysis results for (a) Pa Fm in K-1 well and (b) Pa Fm in L-1 well.

4.4. Principal component analysis

Principal component analysis (PCA) was applied for laboratory and well-logging data derived from Silurian and Ordovician intervals drilled in wells L-1, B-1 and W-1. PCA is a multivariate statistical method used to reduce multidimensional data set into lower dimensions. This mathematical operation helps to extract unobservable variable hidden in the original measurements.

In each analyzed well intervals, results were similar. Three to five principal components (PC) were enough for 70–90% of variance explanation. PCA pointed out that about 50% in W-1 and L-1 wells and 70% in B-1 well of information about the data set were contained in spectral gamma logs, neutron logs and acoustic logs. It meant that the main reason for data diversification was shaliness, clay content and porosity of rocks. The next 20–30% of variance was expressed by density and resistivity logs. These parameters could be treated as porosity and saturation logs. The third PC provided information about the presence of organic matter. This was indicated by the high value of correlation coefficient between PC and uranium log. PCA applied to laboratory data showed that the main variance of the data set was associated with hydrocarbon indicators such as TOC, cation exchange capacity (CEC) and parameters from Rock-Eval measurement, i.e. free hydrocarbons content, S1, and hydrocarbons from cracking process, S2. In the second PC, the highest impact was connected with clay mineral content.

4.5. Cluster analysis

Cluster analysis (CA) was used for grouping data and classification according to natural physical features of rocks. CA pointed out preliminary formation classification and gas-bearing identification. It helped to define zones of interests based on well logs and laboratory data criteria and improved characteristic of shales with gas saturation. Several different hierarchical and non-hierarchical methods for cluster creating were applied. As a result, groups that corresponded to the gas-bearing intervals were selected. Diversification between sweet spots and surrounding beds was shown. Complex analysis showed internal diversification in each gas formation.

The input data included laboratory measurement results and well-logging data. In the first step of CA, data from all Ordovician and Silurian formations were included. Result showed that each cluster aggregated data associated mostly with one formation. It meant that all

http://dx.doi.org/10.5772/67301

lithostratigraphic units had different physical properties and CA could be the first step in the formation identification.

In the second step of analysis, the CA was performed for Ja Mb and Sa Fm independently (**Figure 8**). These formations were treated as potential sweet spot intervals. In each formation, internal heterogeneity was found. Diversity was also observed between the same formations in different wells. For example, in L-1 well, the Ja Mb was divided into four groups, whereas in B-1 well it was divided into five groups. In Sa Fm, four clusters were selected in L-1 well and six in B-1 well. Despite this, in both wells clusters with corresponding parameters could be found. In all wells there were distinguished clusters: (a) with high (about 10% and more) kerogen content, small (0–3%) porosity, high (about 70%) clay minerals and small (about 30%) quartz content; (b) with small (about 3%) kerogen content, high (about 10%) porosity, high (about 70%) clay minerals and small (30%) quartz content; (c) with high (about 8%) kerogen content, porosity in range of 0–10%, comparable content of clay minerals and quartz (d) with high (about 8%) kerogen content, average porosity about 6%, small (about 30%) clay minerals and high (about 70%) of quartz content.

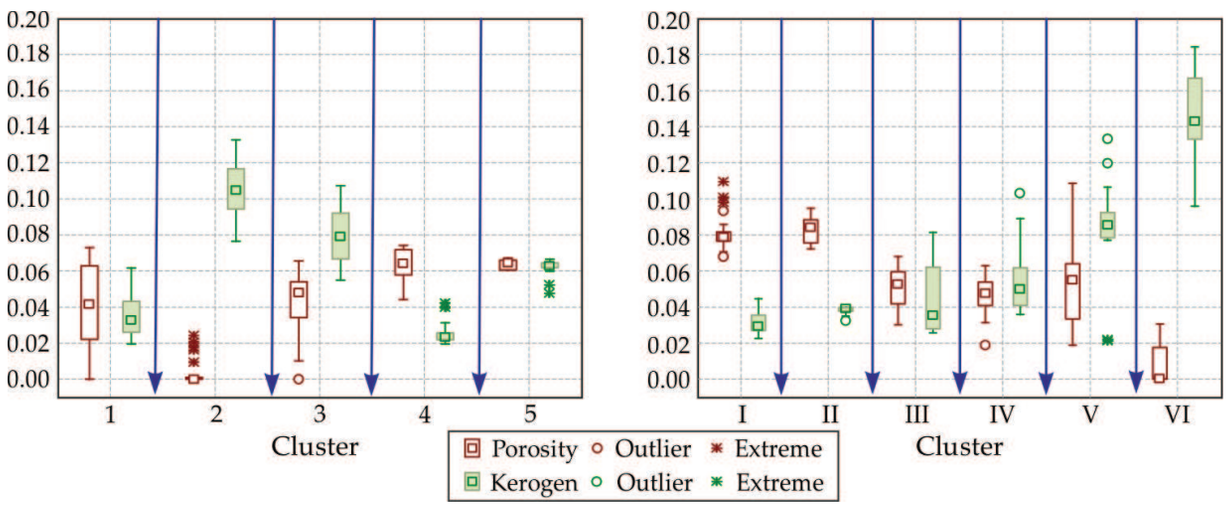

Figure 8. Box plots for porosity and kerogen content in each cluster in Ja Mb (left) and Sa Fm (right), well B-1. Symbols: middle point equals median value, box equals first and third quartile and whiskers equal range of non-outlier values.

Summarizing cluster characterization, CA was a good mathematical tool for fast preliminary Polish shale classification. Sweet spots in Polish shales are inhomogeneous; there are intervals with possible gas presence and without (or very poor) gas saturation.

5. Elastic property modelling of shale gas formations

Clay minerals, important components of shales, influence elastic properties of rocks and their anisotropy [16]. Elastic properties depend not only on mineral composition and percentage of selected compounds but also on shape and orientation of grains. Jones and Wang [17] presented the example of the Cretaceous shales from Williston Basin and the results of the

experimental measurements of five independent components of elasticity vector, C_{11}, C_{33}, C_{44}, C_{66} and C_{13}, which characterize the simplest case of anisotropy of hexagonal symmetry, i.e. transverse isotropy (TI) [18]. In the presented work, a synthetic model of the similar shales with organic matter on the basis of the published data was prepared [19, 20]. Elastic parameter modelling and bulk density calculations were done using the theoretical relations by Kuster and Toksöz [21] applying the differential effective medium (DEM) solution [19]. There were used theoretical models of porous formation by Biot-Gassmann [22, 23] and Kuster-Toksöz and the original software *Estymacja* [15, 24].

5.1. Elastic parameters calculated by *Estymacja* software in L-1 well

An estimation of P- and S-wave velocity and elastic moduli was based on known theoretical formulas of Biot-Gassmann or Kuster-Toksöz [21–23] which describe multiphase media corresponding to rocks with granular structure (grains of solid phase) with porous space saturated with medium (liquid phase or gas phase).

Elastic parameters of rocks are a result of an interaction of all phase components, rock matrix and medium and also depend on the anisotropy of a rock matrix. The *Estymacja* software allows elastic parameters of the rocks and bulk density to be determined from results of the comprehensive interpretation of well-logging data, i.e. volumes of mineral components, porosity and water, gas and oil saturation in the flushed zone or virgin zone [15, 25]. The final results of *Estymacja* software in the form of set of curves illustrating variability of P slowness and S slowness (DTP and DTS, respectively), together with neutron porosity, NPHI, bulk density, RHOB, water saturation, SW, natural radioactivity, GR, logs and lithology and V_P/V_S curves, are presented in **Figure 9**.

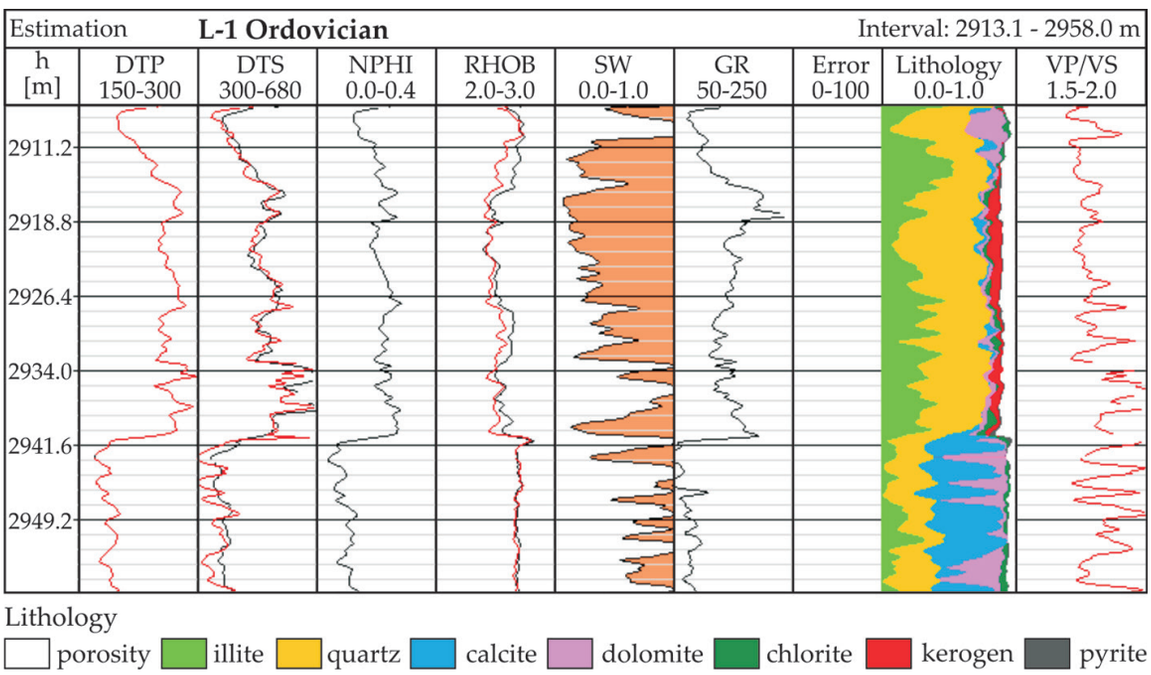

Figure 9. Calculated (red) and measured (black) curves in the Ordovician depth section in L-1 well. *Estymacja* software and Kuster-Toksöz model were used.

http://dx.doi.org/10.5772/67301

5.2. Synthetic model of shale gas formation

Elastic parameters were calculated for the synthetic model of shale gas formation with organic matter in mineral skeleton or in porous space and formation water and gaseous hydrocarbons in pore space. Passey [20] in his model of shale gas rock divided organic matter into three parts: rock matrix, organic matter component and medium in pore space. Increase of compaction caused that grains revealed tendency to horizontal position and organic matter composed subhorizontal lamellae. On the basis of thin sections, it was proved that organic matter (mainly kerogen) was plastic [20]. Primarily, organic matter was located in the matrix and did not fill the pores. When the maturity increased, kerogen was more mobile and could be intruded into pore space. Models of shale gas formation assumed in modelling are presented in **Figure 10**.

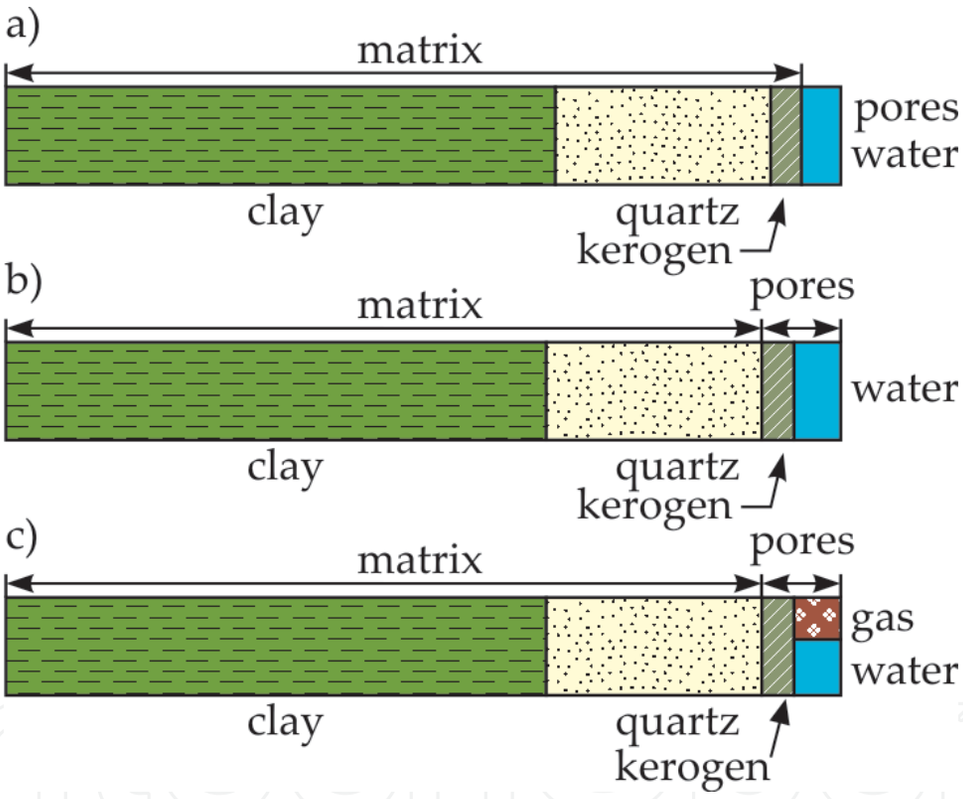

Figure 10. Models assumed in calculations.

In Model 1, it was assumed that clay, quartz and kerogen were present in skeleton; formation water was in pores. Porous spectra were as follows: $\alpha_{water} = 0.05$ and $C(\alpha_{water}) = \Phi = 0.05$ (Φ, porosity) and water parameters $K_W = 2.6$ GPa and $RHOB_W = 1.05$ g/cm^3. In Model 2, it was assumed that kerogen was in porous space with characteristic spectra, $\alpha_{kerogen} = C(\alpha_{kerogon}) = V_{kerogen}$ ($V_{kerogen}$, volume of kerogen) and porous spectra of water, $\alpha_{water} = 0.05$ and $C(\alpha_{water}) = \Phi = 0.05$. In Model 3, it was assumed that kerogen, formation water and gas were located in pores. Velocity of P-waves, V_P, as a function of kerogen volume for Models 1 and 2

is presented in **Figure 11**. Decrease of V_P was visible with increase of kerogen and decrease of volume of shale, V_{sh}, in rock matrix. Similar behaviour was observed for bulk elastic modulus, K, and shear elastic modulus, MI. Calculations were also made in the case when water and gas were present in porous space.

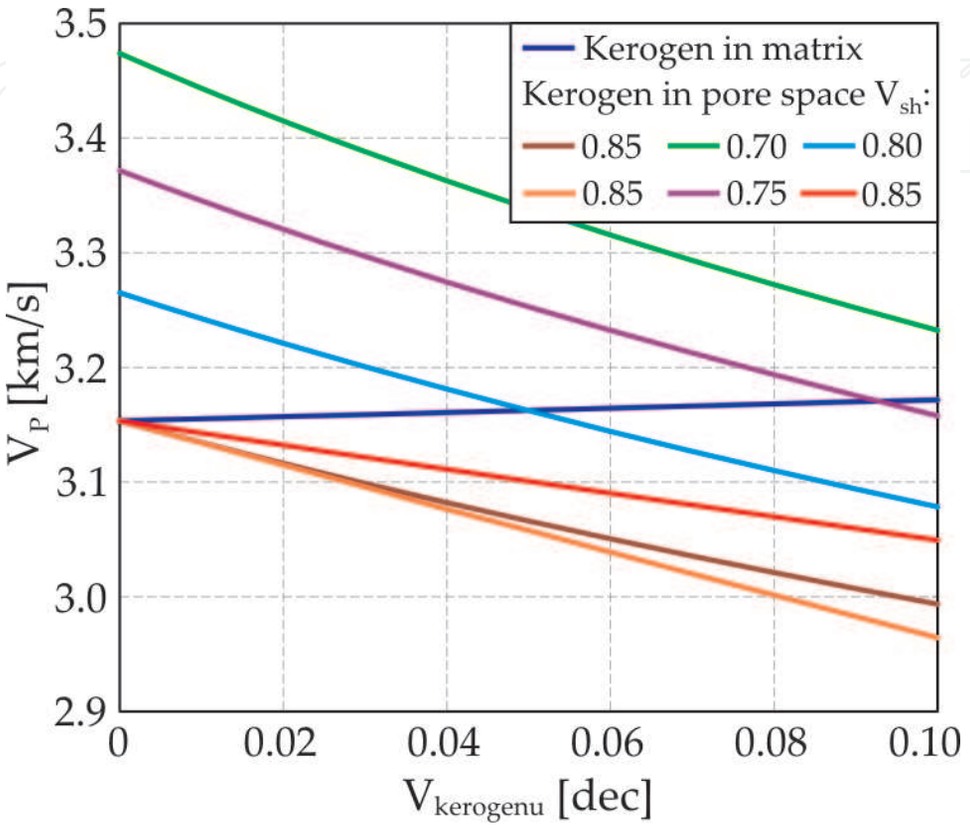

Figure 11. Velocity of P-wave vs. kerogen volume. Model 1 (blue curve) and Models 2 and 3 (other curves). Various kerogen volumes in pore space are marked by different colours.

In Variant 1, it was assumed that water and gas were present in separate pores and pore spectrum was the same: $\alpha_{water} = 0.05$ and $C(\alpha_{water}) = \Phi = 0.05$ and $\alpha_{gas} = 0.05$ and $C(\alpha_{gas}) = \Phi = 0.05$, what meant porosity $\Phi = 0.1$. In Variant 2 it was assumed that water ($S_W = 0.8$) and gas ($S_G = 0.2$) were a mixture. In both cases, a linear decrease of V_P and V_S with kerogen volume increase was observed, but in Variant 2 it was higher. Variability of both waves, velocity $V_S = f(V_P)$ (**Figure 12a**) and acoustic impedance AIS = f(AIP), was also analyzed (**Figure 12b**). Data in the plots were related to depth intervals with gas, formation water or saturated with gas and water from the Silurian and Ordovician formations in the L-1 well. Beds of different gas saturations were distinctly visible: yellow and red points meant high gas saturation, and blue points meant formation water saturation.

5.3. Brittleness of shale gas formation

Mechanical properties of shale gas formations are crucial in hydraulic fracturing for gas production in low permeability reservoirs. Such rocks are characterized by various brittleness

http://dx.doi.org/10.5772/67301

indices [26] which are considered in aspects of mineral composition and elastic properties. Quartz and carbonates in rocks cause increase of brittleness in contrary to shaliness-rich formations where ductile deformations are more frequently observed and skeleton weakness is observed. On the other hand, carbonate cements may limit natural fracture flow ability. High volume of carbonates and presence of swelling clay minerals are the main reasons making difficult production from discussed gas deposits. Young's modulus or Poisson's ratio may be used as measures of brittleness index (BI) (**Figure 13**).

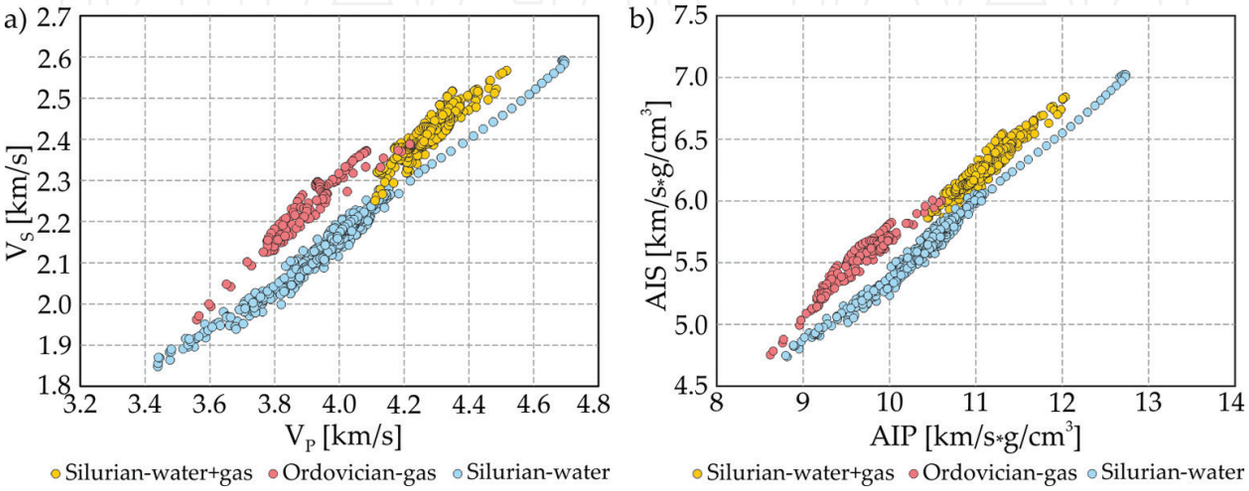

Figure 12. Relationship between velocity V_S vs. V_P and acoustic impedance AIS vs. AIP for the selected depth intervals in L-1 well.

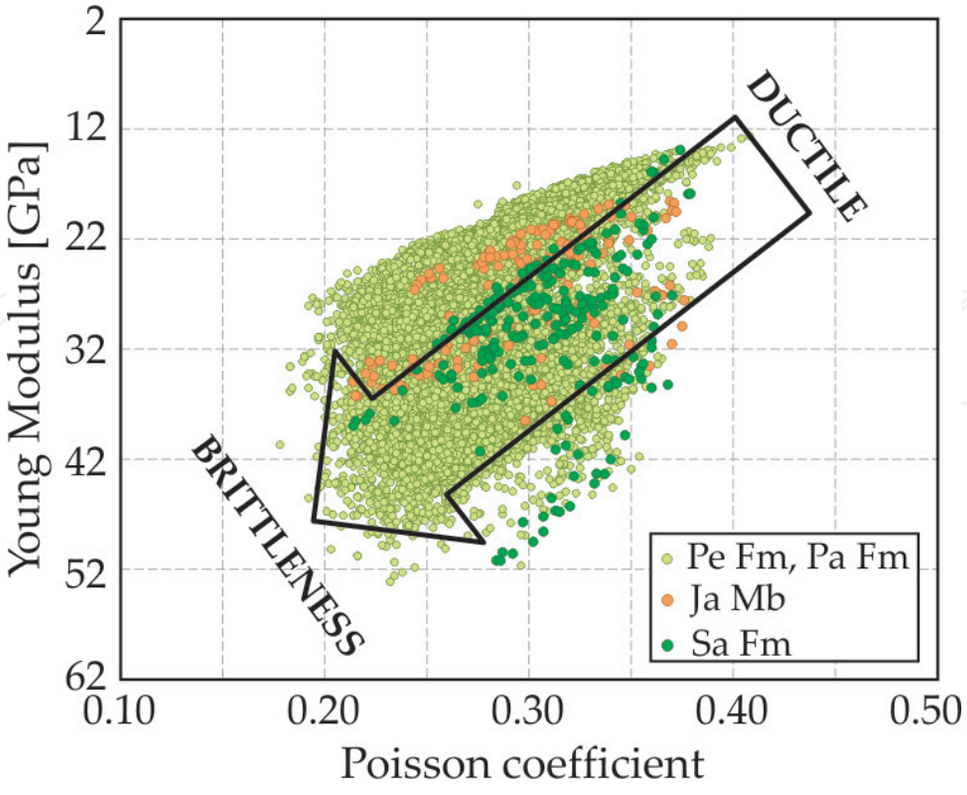

Figure 13. Poisson's ratio vs. Young's modulus, K-1 well.

5.4. Summary of results

Kerogen influenced measured petrophysical parameters, but shaliness and pores geometry were also important in considering this influence. Changeability of elastic parameters was not distinct with the increase of kerogen volume when it composed mineral skeleton; however, when pores were filled with kerogen, variability of elastic parameters increased. Kerogen in pore space caused decrease of velocity of P- and S-waves as well as elastic moduli K and MI. Increase of kerogen volume caused increase of V_P/V_S ratio. V_S vs. V_P and AIS vs. AIP cross plots enabled separation between water-saturated and gas-saturated beds. Shales of higher Young's modulus values and lower Poisson's ratio revealed higher brittleness.

6. Measurements of acoustic emission and volumetric strain during sorption and desorption of CH_4 on shale sample

Acoustic emission (AE) is an elastic wave generated and propagating in the medium as a result of dynamic processes. Generation of a seismo-acoustic signal is a mechanical process, brought about by diverse mechanisms associated with strain and breaking of the medium (opening and closing of pores, dislocation movements proceeding at variable rate, slippage and friction, plastic and nonplastic deformations), structural changes, phase transitions and chemical reactions and temperature changes.

The basic AE parameters include acoustic activity representing the number of impulses (AE counts) registered in an arbitrarily chosen time window, mean signal energy—the ratio of energy emitted within a given time interval to the number of impulses registered in the same time and cumulative energy—total energy of impulses registered from the beginning of record-taking. AE recordings are utilized for forecasting rock bursts and gas and rock outbursts in coal mines [27]. The test stands for acoustic emission measurement [27], and a single-channel device for seismic-acoustic measurements was designed and engineered as a prototype. The main component is a vacuum-pressure chamber, provided with a steel waveguide and six wires for strain measurements. The chamber is connected to gas bottles and a vacuum pump through a system of tubes and pressure-control valves. Measurement data are saved on a computer connected to the system.

The test facility has been modified since time of measurements made for coal [27]. At first, the integrating system in the seismic-acoustic instrumentation, which calculated the surface area of impulses over a given level of discrimination, would split the entire measurement range of 3 V into 10 identical channels, 300 mV each. When the interface was used, the measurement range was extended to 10 V and is now split into 4000 identical channels, 2.5 mV each. This solution provides a higher resolution energy data; hence, the results give more information about events and allow for detecting even low-energy events. The measuring path allows for monitoring AE impulses in the frequency range from 100 Hz to 1 MHz, with the option for frequency band setting. Within this band single events are detected, and the integral of the positive portion of the measured plot is obtained accordingly. The key component of the measurement circuit is a piezoelectric sensor. Four RL strain gauges were fixed on a shale sample, which was then attached to the waveguide in the pressure-vacuum chamber. Measurement cycles were conducted at the

http://dx.doi.org/10.5772/67301

frequency of one per minute. The signal resolution was of the order of 0.001%. The observed acoustic emission patterns do not resemble those registered for coal samples (**Figure 14**) [28].

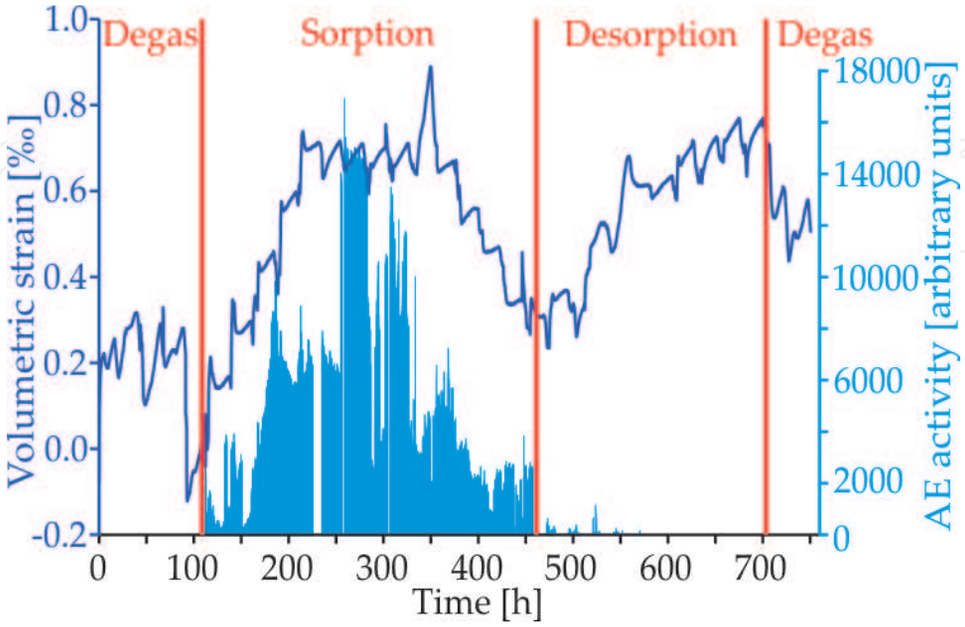

Figure 14. Acoustic emission and volumetric strain registered on a shale sample during the sorption of CH_4.

In the case of coal samples, the process of AE data acquisition was much faster. Strains measured in the shale were lower by one order of magnitude than those registered for coal, and their variability pattern was different, too. Volumetric strains increased for about 150 h of the sorption process, including the stage of stabilization (around the 100th hour), followed by a strain decline, which was never observed for coal. The analysis of registered strain data revealed that they should be recorded for longer time during sorption. The general conclusion can be drawn that sorption processes in shale are much slower than in coals.

7. Final remarks

Presented results show that Polish shale formations of the Silurian and Ordovician age are different as regards mineral composition, reservoir properties and elastic parameters. In each formation internal heterogeneity was found. Diversity was also observed within the same formations in different wells. Two selected formations were recognized as potential sweet spots, i.e. Ja Mb and Sa Fm. They are relatively rich in organic matter. Results of the analyses indicate distinctly visible differences between them and surrounding formations (Pe Fm, Pa Fm and Pr Fm).

Applied statistical analyses, i.e. simple statistics, histograms, box plots and also factor analysis, principal component analysis and cluster analysis show themselves as useful tools for proving diversity of shale formations in the study. Research based on the laboratory results, well logs and the outcomes of the comprehensive interpretation of well logging confirmed great diversification of formations in the study but also revealed some regularities. Factor analyses

and principal component analyses enabled limitation of great number of logs saving the necessary information to make classification.

Elastic property modelling using theoretical models and results of the comprehensive interpretation of well logs provided estimated velocity of P- and S-waves and bulk density in all wells and helped in completing indispensable information about brittleness of shale gas formations.

Preliminary results of acoustic emission investigations show additional characteristic features of shale gas rock and revealed that acoustic emission and volumetric strain of a shale sample induced by the sorption processes are lower for shale than for coals.

Methodology of laboratory measurements, well data acquisition and processing was only slightly fitted to specific features of shale rocks. Majority of measurements were typical for prospection of conventional hydrocarbon reservoirs. In spite of it, selection of potential sweet spots among adjacent beds was a success.

Acknowledgements

This study was financed by the National Centre for Research and Development in the programme Blue Gas project, 'Methodology to determine sweet spots based on geochemical, petrophysical and geomechanical properties in connection with correlation of laboratory test with well logs and generation model 3D' (MWSSSG) Polskie Technologie dla Gazu Łupkowego. Data for the study were delivered by Polish Oil and Gas Company, Warsaw, Poland. Statistica 12 software was used under the AGH UST grant from StatSoft. Plots and figures were prepared by Teresa Staszowska.

Author details

Jadwiga A. Jarzyna*, Maria Bała, Paulina I. Krakowska, Edyta Puskarczyk, Anna Strzępowicz, Kamila Wawrzyniak-Guz, Dariusz Więcław and Jerzy Ziętek

*Address all correspondence to: jarzyna@agh.edu.pl

Faculty of Geology, Geophysics and Environmental Protection, AGH University of Science and Technology, Krakow, Poland

References

[1] Kiersnowski H. Geological environment of gas-bearing shales. In: Nawrocki J., editor. Shale Gas as Seen by Polish Geological Survey. Polish Geological Institute – National Research Institute; Warsaw. 2013. pp. 26-31.

[2] Wawrzyniak-Guz K., Jarzyna J.A., Zych M., Bała M., Krakowska P.I., Puskarczyk E. Analysis of the heterogeneity of the Polish shale gas formations by Factor Analysis on the basis of well logs. In: Extended Abstract of the 78th EAGE Conference and Exhibition 2016; 30 May–2 June 2016; Vienna. 2016. p. Tu SBT3 07.

[3] Poprawa P. Shale gas potential of the Lower Palaeozoic complex in the Baltic and Lublin-Podlasie basins (Poland) (in Polish). Przegląd Geologiczny. 2010;**58**(3):226-249.

[4] Więcław D., Kotarba M.J., Kosakowski P., Kowalski A., Grotek I. Habitat and hydrocarbon potential of the lower Paleozoic source rocks in the Polish part of the Baltic region. Geological Quarterly. 2010;**54**(2):159-182.

[5] Karcz P., Janas M., Dyrka I. Polish shale gas deposits in relation to selected shale gas perspective. Przegląd Geologiczny. 2013;**61**(11/1):608-620.

[6] Porębski S.J., Prugar W., Zacharski J. Silurian shales of the East European Platform in Poland – some exploration problems. Przegląd Geologiczny. 2013;**61**(11/1):630-638.

[7] Podhalańska T. Late Ordovician to Early Silurian transition and the graptolites from Ordovician/Silurian boundary near the SW rim of the East European Craton (northern Poland). Series Geological Correlation. 2003;**18**:165-172.

[8] Tomczyk H. Stratigraphic problems of the Ordovician and Silurian in Poland in the light of recent studies (in Polish). Prace Państwowego Instytutu Geologicznego. 1962;**35**:1-134.

[9] Podhalańska T. Graptolites – stratigraphic tool in the exploration of zones prospective for the occurrence of unconventional hydrocarbon deposits. Przegląd Geologiczny. 2013;**61**(11/1):621-629.

[10] Modliński Z., Szymański B., Teller L. The Silurian lithostratigraphy of the Polish part of the Peri-Baltic Depression (N Poland) (in Polish). Przegląd Geologiczny. 2006;**54**(9):787-796.

[11] Modliński Z., Szymański B. The Ordovician lithostratigraphy of the Peribaitic Depression (NE Poland). Geological Quarterly. 1997;**41**(3):273-288.

[12] Modliński Z., Szymański B. Lithostratigraphy of the Ordovician in the Podlasie Depression and the basement of the Płock–Warsaw Trough (eastern Poland) (in Polish). Biuletyn Państwowego Instytutu Geologicznego. 2008;**430**(430):79-112.

[13] Brindle S., O'Connor D., Windmill R., Wellsbury P., Oliver G., Spence G., et al. An integrated approach to unconventional resource play reservoir characterization, Thistleton-1 case study, NW England. First Break. 2015;**33**(2):79-86.

[14] Data available for the project Blue Gas financed by the National Centre for Research and Development: Methodology to determine sweet spots based on geochemical, petrophysical and geomechanical properties in connection with correlation of laboratory test with well logs and generation model 3D (MWSSSG) Polskie Technologie dla Gazu Łupkowego. 2013-2016. Data for the study were allowed by Polish Oil and Gas Company, Warsaw, Poland.

[15] Bała M., Cichy A. Comparison of P- and S-waves velocities estimated from Biot-Gassmann and Kuster-Toksöz models with results obtained from acoustic wavetrains interpretation. Acta Geophysica. 2007;**55**(2):222-230. DOI: 10.2478/s11600-007-0006-6

[16] Katahara K.W. Clay minerals elastic properties. In: Expanded Abstracts of the 66th Annual International Meeting SEG; 10-15 November 1996; Denver, Colorado. 1996. pp. 1691-1694.

[17] Jones L.E.A., Wang H.F. Ultrasonic velocities in Cretaceous shales from the Williston basin. Geophysics. 1981;**46**(3):288-297. DOI: 10.1190/1.1441199

[18] Thomsen L. Weak elastic anisotropy. Geophysics. 1986;**51**(10):1954-1966. DOI: 10.1190/1.1442051

[19] Mavko G., Mukerji T., Dvorkin J. The Rock Physics Handbook: Tools for Seismic Analysis of Porous Media. 2nd ed. Cambridge: Cambridge University Press; 2009. 511 p. DOI: 10.1017/CBO9780511626753

[20] Passey Q.R., Creaney S., Kulla J.B., Moretti F.J., Stroud J.D. A practical model for organic richness from porosity and resistivity logs. AAPG Bulletin. 1990;**74**(12):1777-1794.

[21] Kuster G.T., Toksöz M.N. Velocity and attenuation of seismic waves in two-phase media: part I. Theoretical formulations. Geophysics. 1974;**39**(5):587-606. DOI: 10.1190/1.1440450

[22] Biot M.A. Mechanics of deformation and acoustic propagation in porous media. Journal of Applied Physics. 1962;**33**(4):1482-1498. DOI: 10.1063/1.1728759

[23] Gassmann F. Elastic waves through a packing of spheres. Geophysics. 1951;**16**(4):673-685. DOI: 10.1190/1.1437718

[24] Bała M. Effect of water and gas saturation in layers on elastic parameters of rocks and reflection coefficients of waves. Acta Geophysica Polonica. 1994;**42**(2):49-158.

[25] Jarzyna J., Bała M., Cichy A. Elastic parameters of rocks from well logging in near surface sediments. Acta Geophysica. 2010;**58**(1):34-48. DOI: 10.2478/s11600-009-0036-3

[26] Grieser W.V., Bray J.M. Identification of production potential in unconventional reservoirs. In: SPE Conference Paper of the Production and Operations Symposium; 31 March–3 April 2007; Oklahoma City, Oklahoma. Society of Petroleum Engineers. 2007. p. SPE-106623-MS. DOI: 10.2118/106623-MS

[27] Majewska Z., Ziętek J. Acoustic emission and sorptive deformation induced in coals of various rank by the sorption-desorption of gas. Acta Geophysica. 2007;**55**(3):324-343. DOI: 10.2478/s11600-007-0022-6

[28] White C.M., Smith D.H., Jones K.L., Goodman A.L., Jikich S.A., LaCount R.B., et al. Sequestration of carbon dioxide in coal with enhanced coalbed methane recovery – a review. Energy & Fuels. 2005;**19**(3):659-724. DOI: 10.1021/ef040047w